JOURNAL OF APPLIED ELECTROCHEMISTRY 18 (1988) 225–231

Corrosion inhibition study of a carbon steel in acidic media containing hydrogen sulphide and organic surfactants

N. PEBERE, M. DUPRAT†, F. DABOSI

UA CNRS 445, Laboratoire de Métallurgie Physique, ENS Chimie, 118 Route de Narbonne, 31077 Toulouse Cedex, France

A. LATTES

UA CNRS 470, Laboratoire des IMRCP Université Paul Sabatier, 118 Route de Narbonne, 31062 Toulouse Cedex, France

A. DE SAVIGNAC

UA CNRS 470 and INSAT, Avenue de Rangueil, 31077 Toulouse Cedex, France

Received 16 March 1987; revised 14 September 1987

Inhibition of the corrosion of a carbon steel (0.4% C) by 2-hexadecyl imidazoline and 2-hexadecyl imidazole has been evaluated by electrochemical techniques and correlated with surface tension measurements. Plots of inhibitor efficiency versus surfactant concentration produce S-shaped curves which are assumed to represent adsorption isotherms. A sharp increase in slope was observed at concentrations below the critical micellar concentration. This increase in slope is accounted for by changes in conformation of the adsorbed molecules: horizontal orientations (with respect to the surface) at lower concentrations reflecting cathodic behaviour and perpendicular orientations at the higher concentrations reflecting mixed cathodic and anodic behaviour. At increasing concentrations the inhibitory effect remained constant, suggesting complete saturation of the surface in a bilayered arrangement. Electrochemical impedance measurements, carried out for concentrations greater than the critical micellar concentration, corroborate this assumption: the inhibitors form a thick but adherent micellar film which acts as a diffusion barrier.

1. Introduction

Organic surfactants are commonly employed as corrosion inhibitors on iron and steel. In previous studies [1–3] we have shown that there is a relationship between inhibitory properties of certain compounds (alkylamines, alkylimidazoles, alkylimidazolines) and their hydrophobic character. An increase in inhibitory action was observed when the concentration of surfactant in the corrosive solution approaches the critical micellar concentration (CMC). Above this value there was no further increase in efficiency which remains constant for further increases in surfactant concentration.

For a family of molecules which only differ in length of carbon chain, the inhibitory action obeys Traube's rule [4] for values of hydrophobicity corresponding to chain lengths of less than 11-12 methylene groups. Above these chain lengths, this rule is no longer observed, and the inhibitory action either decreases or remains the same depending on the type of molecule.

In the present study, surfactant adsorption at the metal-solution interface (evaluated from steady-state current-voltage curves) was related to the surface tension at the air-solution interface. Electrochemical impedance measurements were also performed under various polarization conditions in order to estimate the anodic and cathodic contributions to the corrosion kinetics in the presence of inhibitors. Two inhibitors were chosen from those studied in previous experiments: 2-hexadecyl imidazoline and 2-hexadecyl imidazole. These compounds have:

a carbon chain long enough to produce strong hydrophobic interactions. They belong to the category of compounds which do not obey Traube's rule. Above the critical value they have a constant efficiency;

polar regions differing essentially in the number and delocalization of π electrons. Differences in inhibitory effects may be interpreted in terms of this property.

2. Experimental details

Experiments were carried out using cylindrical N80 type carbon steel (0.4% C) samples. A thermoretractable sheath prevented the cylindrical area from contact with the solution, the electrode surface area thus

† Deceased September 4, 1986.

0021-891X/88 $03.00 + .12

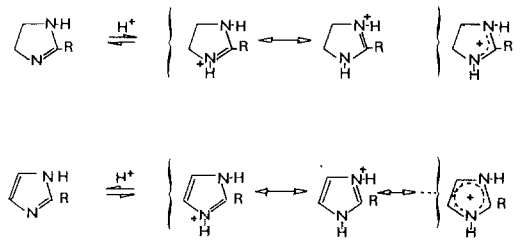

Fig. 1. Protonation and limiting resonant form of 2-hexadecyl imidazoline (above) and 2-hexadecyl imidazole (below).

being only the cross section (1 cm^2). The surface was polished with emery paper (grade 80) then dried in pulsed warm air after an ultrasonic washing in ethanol.

A saturated calomel electrode (SCE) connected through a salt bridge was used as the reference electrode. The auxiliary electrode was a platinum leaf of large area. The corrosive medium was a 5 gl^{-1} solution of ammonium chloride, deoxygenated with high purity nitrogen and saturated by hydrogen sulphide (pH = 4). The solution was stirred mechanically with a Teflon stirrer. The working electrode was introduced by an intermediate device, before being inserted into the cell. Since the two inhibitors used were not completely soluble in this medium, they were employed in solution in ethanol (10% with respect to the total volume). At pH = 4, imidazole (pKa = 7) and imidazoline (pKa = 10.8) are mainly in acid form (Fig. 1) and do not undergo hydrolysis [5]. The electrochemical impedance measurements were performed using small amplitude sine wave signals by means of frequency response analysers Schlumberger-solartron 1174 and 1250 in a frequency range from 100 kHz to several mHz with five points per decade. The whole experimental set-up has been fully described elsewhere [6].

3. Results

3.1. *Determination of the critical micellar concentrations*

At 25° C, which is above the Krafft point [2], the interfacial tensions, γ, of 2-hexadecyl imidazoline and 2-hexadecyl imidazole were determined by the ring detachment method under identical conditions to those used for measurement of corrosion currents. The values of the critical micellar concentration (CMC) were (2.5 $\pm$ 0.25) $\times$ 10^{-5} M and (5 $\pm$ 0.5) $\times$ 10^{-6} M for 2-hexadecyl imidazoline and 2-hexadecyl imidazole respectively (Figs 2 and 3).

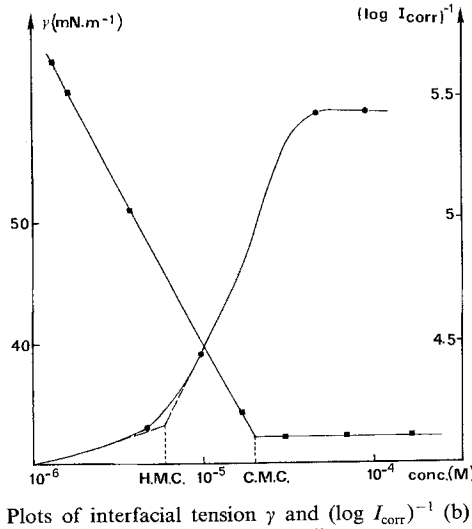

Fig. 2. Plots of interfacial tension γ and $(\log I_{corr})^{-1}$ (b) against concentration C for 2-hexadecyl imidazoline.

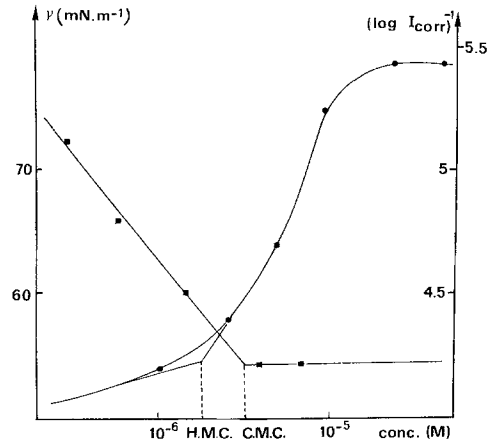

Fig. 3. Plots of interfacial tension γ and $(\log I_{corr})^{-1}$ (b) against concentration C for 2-hexadecyl imidazole.

3.2. *Steady-state cathodic current-voltage curves*

The plots of log I versus E (Figs 4 and 5) were determined in the potentiostatic mode. The curves were plotted after equilibration for 30 min at the corrosion potential with constant agitation.

From these results it was observed that:

(1) The corrosion current density, I_{corr}, falls with increasing inhibitor concentration, reaching a value of 4 $\mu A/cm^2$ corresponding to 96% protection. Displacement of the corrosion potential towards anodic potentials is in agreement with the inhibitory effects observed.

(2) The high inhibitory efficiencies observed at 5 $\times$ 10^{-5} M for 2-hexadecyl imidazoline and at 10^{-5} M for 2-hexadecyl imidazole are at concentrations above the critical micellar concentration. Corrosion cur-

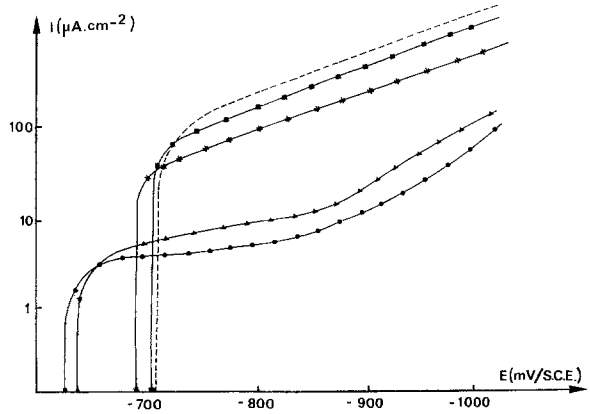

Fig. 4. Steady-state cathodic current-voltage curves at various concentrations of 2-hexadecyl imidazoline. Preliminary hold time at E_{corr} of 30 min. N80 carbon steel/5 gl^{-1} NH_4Cl deaerated and saturated by H_2S. Blank solution: (■) 5 $\times$ 10^{-6} M; (*) 1 $\times$ 10^{-6} M; (▲) 2 $\times$ 10^{-5} M; (●) 5 $\times$ 10^{-5} M.

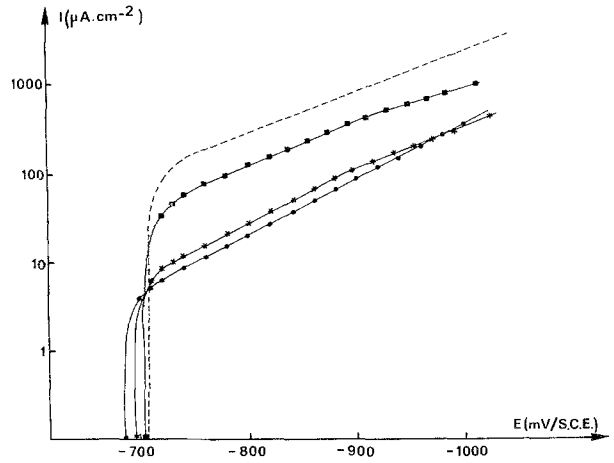

Fig. 5. Steady-state cathodic current-voltage curves at various concentrations of 2-hexadecyl imidazole. Preliminary hold time at E_{corr} of 30 min. N80 carbon steel/5 g l^{-1} NH_4Cl deaerated and saturated by H_2S. Blank solution: (■) 2.5×10^{-6} M; (*) 1×10^{-5} M; (●) 5×10^{-5} M.

rent densities then remain stable with increasing concentration.

(3) When the concentrations reach values close to the CMC, the current-voltage curves are modified, indicating a change in the mode of action of the compounds:

(a) this is essentially cathodic for low inhibitor concentrations, a reduction in current density with no change in slope is observed;

(b) it is mixed anodic and cathodic action for high concentrations ($C > 10^{-5}$ M for 2-hexadecyl imidazoline and $> 5 \times 10^{-6}$ M for 2-hexadecyl imidazole).

3.3. *Steady-state anodic current-voltage curves*

The steady-state current-voltage curves in the anodic range in solutions containing 5×10^{-5} M of 2-hexadecyl imidazoline and 2-hexadecyl imidazole are shown in Fig. 6.

A comparison of curves (a), (b) and (c) shows that the addition of the compounds increases the overvoltage in the immediate vicinity of the corrosion potential. This effect is more marked with 2-hexadecyl imidazoline. However, for high overpotentials it is difficult to reach steady-state conditions.

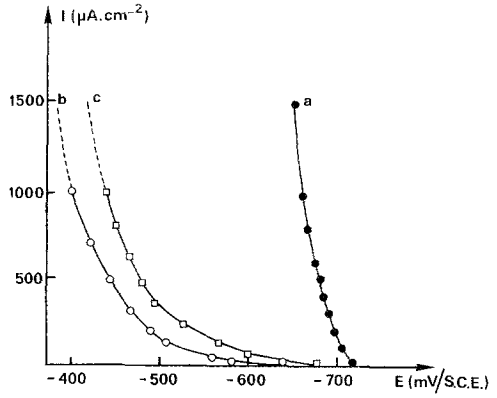

Fig. 6. Steady-state anodic current voltage curves; N80 carbon steel/5 g l^{-1} NH_4Cl deaerated and saturated by H_2S. (a) Blank solution; (b) with 5×10^{-5} M of 2-hexadecyl imidazoline; (c) with 5×10^{-5} M of 2-hexadecyl imidazole.

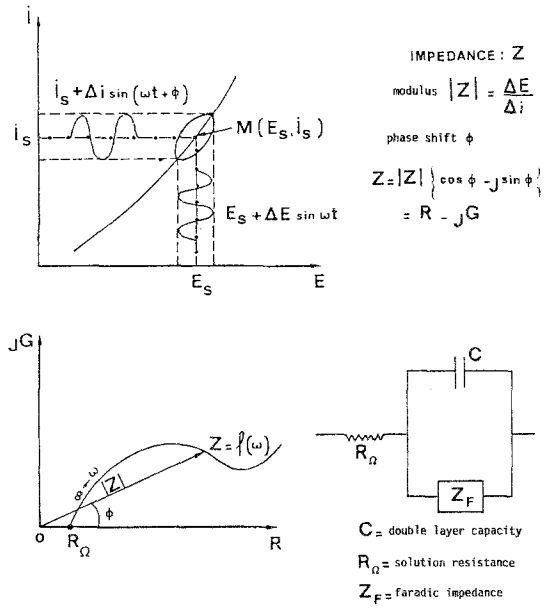

Fig. 7. Basic principles for determining electrochemical impedance.

3.4. *Electrochemical impedance measurements*

The electrochemical impedance was determined by a method of low perturbation which allowed the studied system to remain in a state close to its initial state. Using a sine wave signal, the impedance $Z = \Delta E/\Delta I$ is defined, at each point of the steady-state current-voltage curve, as indicated in Fig. 7. Impedance measurements may be plotted in the complex plane ($R - jG$) as a function of the frequency.

If it is assumed that the double layer component, C, of the overall impedance, Z, can be separated from the faradaic component, Z_F, the interface behaviour can thus be represented by the electrical equivalent circuit shown in Fig. 7, where R_Ω takes into account the existence of the electrolytic resistance. From this electrical equivalent circuit, it appears that the high frequency limit of the impedance gives R_Ω, while the low frequency limit gives the sum ($R_\Omega + R_p$). R_p corresponds, in this case, to R_p true and is equal to the slope of the steady-state current-voltage curve.

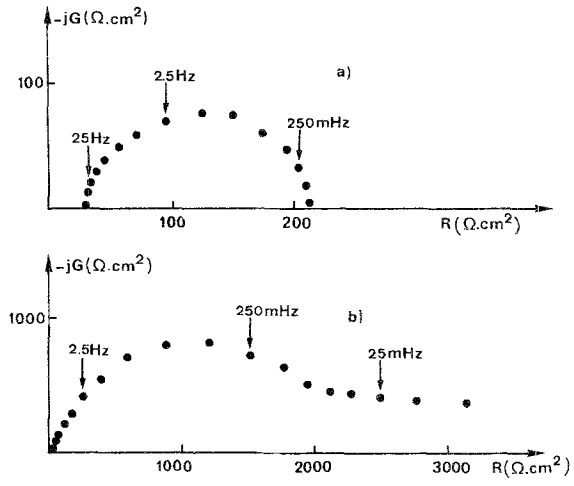

Fig. 8. Electrochemical impedance diagram determined in galvanostatic mode at $I = 0$; (a) 5 g l^{-1} $NH_4Cl + H_2S$; (b) 5 g l^{-1} $NH_4Cl + H_2S + 5 \times 10^{-5}$ M of 2-hexadecyl imidazoline.

Table 1. The values of the main parameters of the impedance diagrams

Test media	R_T (Ωcm^2)	f_c (Hz)	C ($\mu F/cm^2$)
Carbon steel/5 $g l^{-1}$ NH_4Cl + H_2S	200 ± 5	1.6 ± 0.2	500 ± 80
Carbon steel/5 $g l^{-1}$ NH_4Cl + H_2S + 5 × 10^{-5} M of 2-hexadecyl imidazoline	2200 ± 100	0.25 ± 0.05	300 ± 80

3.4.1. Interface N80/5 $g l^{-1}$ NH_4Cl + H_2S + 5 × 10^{-5} M of 2-hexadecyl imidazoline. The electrochemical impedance diagram determined at the corrosion potential in the galvanostatic mode is shown in Fig. 8b. In comparison with the uninhibited situation (Fig. 8a), an additional capacitive part is observed in the low frequency range, which corroborates the modification mechanism previously evidenced from steady-state data. The values of the main parameters of the impedance diagrams are reported in Table 1. The capacitance C was roughly estimated, since the HF loop is not centered on the real axis, by the relationship $C = (2\pi f_c R_T)^{-1}$ (f_c corresponds to the maximum value of the imaginary component and R_T is the diameter of the loop). The inhibitive efficiency of the compound seems to be characterized by an increase in the diameter of the HF loop and a decrease in the value of the associated capacity (in comparison with the uninhibited solution).

In the cathodic potential range, the impedance diagram exhibited a straight line with a slope equal to 1 which reveals the existence of a Warburg type impedance characteristic of a mass transport relaxation process [7]. This observation is in agreement with the plateau obtained on the steady-state cathodic current-voltage curves. In the anodic potential range, a.c. impedance spectra were reduced to one single capacitive loop. The diameter of this loop decreased while the characteristic frequency increased when the applied current increased. It has been possible to determine, for $60 < I_a < 400\,\mu A\,cm^{-2}$ a nearly constant value of the product I_a by the diameter of the loop and therefore to identify this diameter with R_T

$$R_T I_a = 72 \pm 2\,mV$$

This product can be related to the anodic b_a Tafel slope by the following relationship:

$$2.3 R_T I_a = b_a$$

The value of b_a determined in this way is similar to those obtained from the steady-state current voltage-curve (b_a = 170 mV/dec).

In Fig. 9, numerical values of capacitances were given at different anodic current densities between 0 and 800 $\mu A/cm^2$ in a 5 $g l^{-1}$ ammonium chloride solution containing hydrogen sulphide and 2-hexadecyl imidazoline (5 × 10^{-5} M). The curve shows an increase of the capacitance above 600 $\mu A/cm^2$. The modification of the impedance diagram (Fig. 9) showed two ill-separated capacitive loops and an inductive one. Here, the most plausible assumption is the desorption of the inhibitor for high overpotentials.

Corrosion rate can be determined from impedance data by applying the Stern and Geary relationship [15]. For comparison purposes we have also determined the corrosion rate values from steady state current-voltage curves. The results obtained are reported in Table 2. The examination of this table showed a fairly good agreement between the corrosion rate values determined by the two methods.

3.4.2. Interface N80/5 $g l^{-1}$ NH_4Cl + H_2S + 5 × 10^{-5} M of 2-hexadecyl imidazole. The electrochemical impedance diagram determined at the corrosion

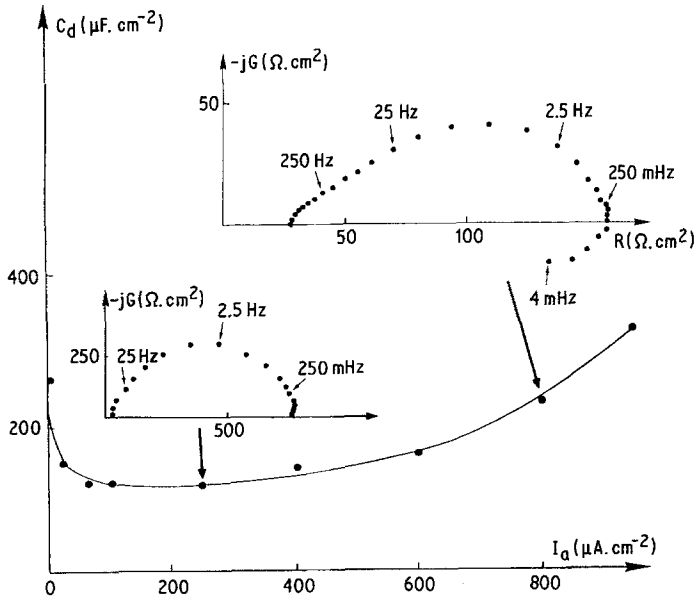

Fig. 9. Evolution of the double layer capacitance at different anodic current densities; N80 carbon steel/ 5 $g l^{-1}$ NH_4Cl deaerated + H_2S + 5 × 10^{-5} M of 2-hexadecyl imidazoline.

Table 2. Comparison of the values of the corrosion rate obtained by different methods. 5 g l^{-1} NH_4Cl + H_2S + 5 × 10^{-5} M of 2-hexadecyl imidazoline

Method	I_{corr} (μA cm^{-2})
Cathodic diffusion plateau	4 ± 1
Extrapolation of the anodic Tafel line	8 ± 2
Impedance measurements	6 ± 1
R_T from impedance measurement, b_a from current-voltage curve	5 ± 1

potential in the potentiostatic mode $I = 0$ and in the presence of 2-hexadecyl imidazole (5×10^{-5} M) exhibited one apparent capacitive loop whose characteristic frequency was very low (~ 25 mHz) (Fig. 10). Extrapolation of BF zone on the real axis results in value ($R_p + R_\Omega$). The polarization resistance value thus determined (~ 3400 Ω cm^2) corresponds to slope $(dE/dI)_{I\to 0}$ of the steady-state current-voltage curve. Nevertheless in the HF range, a linear part with a slope of nearly one was observed. Moreover in the representation log $G = f(\log \omega)$ (ω being the pulsation of the sine wave) a straight line with a slope equal to 0.52 was seen (Fig. 11). This observation reveals the existence in the HF range of a Warburg type impedance. The capacitance C has been estimated from the relationship $C = (R_p\omega_c)^{-1}$ where R_p is the diameter of the loop. The capacitance value appears abnormally high (~ 2000 μF/cm^2).

Such behaviour has been previously observed for corrosion inhibition of a carbon steel in neutral media by monoalkylphosphonate [8]. The observed capacitive loop is not representative of one single time constant. Thus, Fig. 10 represents the cumulative contribution of the mass transport (cathodic) process and the (anodic) charge transfer process. In fact the measured capacitance does not have the physical character of an interfacial capacitance. Any loop can be clearly attributed to the charge transfer process and therefore the corrosion rate cannot be determined from the polarization resistance measurement.

At low cathodic overpotentials, at the onset of the diagram, Warburg impedances are always observed. However where high overpotentials are concerned the impedance spectra show two poorly separated capacitive loops (Fig. 12). The capacitance associated

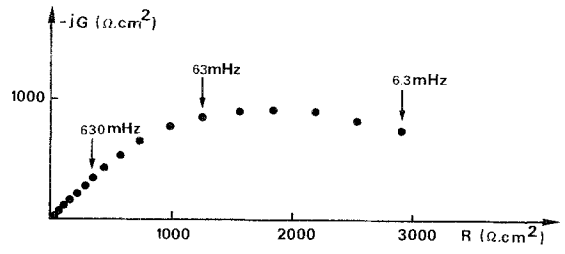

Fig. 10. Electrochemical impedance diagram determined in galvanostatic mode at $I = 0$; N80 carbon steel/5 g l^{-1} NH_4Cl deaerated + H_2S + 5 × 10^{-5} M of 2-hexadecyl imidazole.

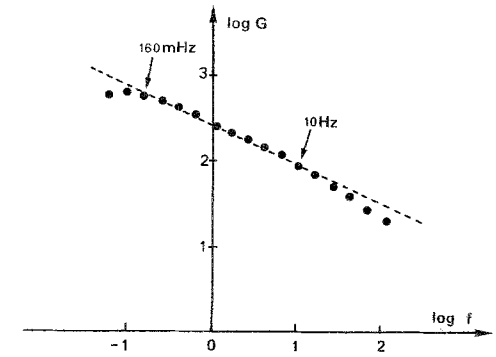

Fig. 11. Log $G = f(\log f)$ representation of the HF part of the impedance diagram presented in Fig. 10.

with the first loop is calculated by the formula:

$$C_d = \frac{1}{2\pi f} \times \frac{b}{(a - R_\Omega)^2 + b^2}$$

(a and b are the real and imaginary parts of the impedance calculated at the frequency f), in a frequency range from 2.5 kHz to 25 Hz (Table 3). This loop appears to be representative of the charge transfer and therefore the decrease of the capacitance with applied overpotential signifies a strengthening of the inhibitor film. In the anodic range, the diameter of the loop decreases when the overpotential is increased whereas the value of the associated capacity greatly decreases.

4. Discussion and conclusions

Corrosion inhibition may be associated with three main types of interfacial effect.

(1) blockage of corrosion sites by adsorption of inhibitory molecules;

(2) hydrophobic effects occurring in the formation of the adsorbed layer;

(3) dielectric effects due to the presence of chemical species in the electrical double layer, which alters its capacitance.

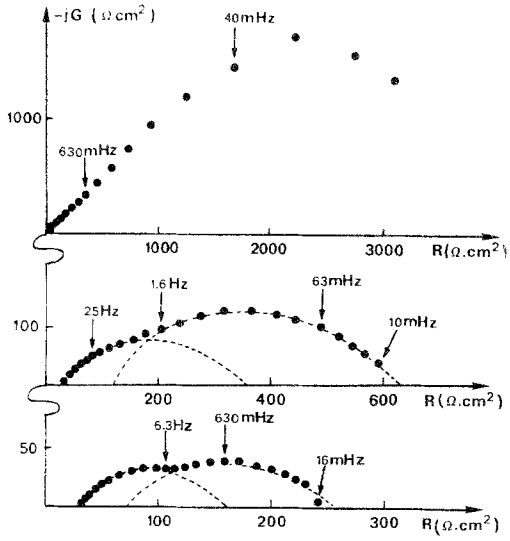

Fig. 12. Electrochemical impedance diagram corresponding to potentiostatic regulation at different cathodic overpotentials. N80 carbon steel/5 g l^{-1} NH_4Cl deaerated + H_2S + 5 × 10^{-5} M of 2-hexadecyl imidazole. From top to bottom: −780, −900, −1020 mV/SCE.

Table 3. Variations of different parameters deduced from the impedance diagrams in the cathodic range. 5 g l^{-1} NH_4Cl + H_2S + 5 × 10^{-5} M of 2-hexadecyl imidazole

E (mV/SCE)	I (μA/cm^2)	R'_1 (Ω cm^2)	f_c (Hz)	C'_1 (μF/cm^2)	R'_2 (Ω cm^2)	f_c (Hz)	C'_2 (μF/cm^2)
−680	0						
−725	5	Capacitive behaviour					
−780	15	Capacitive behaviour					
−860	70	Warburg			800 ± 50	0.125 ± 0.005	1600 ± 200
−900	120	240 ± 10	7 ± 2	130 ± 40	520 ± 20	0.24 ± 0.02	1300 ± 150
−940	200	195 ± 5	8 ± 1	105 ± 15	370 ± 10	0.4 ± 0.05	1100 ± 100
−980	300	140 ± 10	13 ± 3	94 ± 28	235 ± 5	0.45 ± 0.05	1500 ± 200
−1020	450	110 ± 10	25 ± 5	62 ± 18	155 ± 5	0.95 ± 0.05	1100 ± 100

Information on the first and second effects may be obtained from adsorption isotherms and current-voltage curves. In the following discussion we will assume that the plots of $(\log I_{corr})^{-1} = f \log (C)$ (Figs 2 and 3) can be considered as adsorption isotherms [9].

As a first approximation, the known mechanisms of adsorption of ionic organic surfactants on charged interfaces (quartz, silica) can be used to explain the adsorption of corrosion inhibitors. However, the processes involved in the systems studied here are more complex.

Firstly, the metal surface is highly heterogeneous and contains adsorption sites of widely differing affinities for the inhibitor. As corrosion proceeds, anodic and cathodic sites appear. In addition, various species are pre-adsorbed: H_2O, NH_4^+, Cl^-, SH^-, H_2S and poorly defined corrosion compounds are produced.

Secondly, various types of adsorption can take place: (a) competitive adsorption: the inhibitor replaces molecules or ions already present on the surface of the electrode. This is a process of chemisorption due to bonding by the free electron pairs or the π electrons of the surfactant; (b) cooperative adsorption with previously adsorbed species.

Lastly, the net charge of the electrode at the given potential is not easily determined and depends largely on the nature of the pre-adsorbed species. Since cationic surfactants were involved in the present experiments, it can be assumed that the net charge of the electrode (covered with substances other than the inhibitor) was negative.

With reference to these remarks, the results obtained can be interpreted in terms of the concepts of hemimicelles and admicelles introduced by Fuerstenau [10] and Schechter [11]. According to Fuerstenau, hemimicelles are formed on the surface by perpendicular adsorption of surfactant molecules at very low surfactant concentrations. This concept is based on the presence of a sharp increase in slope of the adsorption isotherm. The concentration at the discontinuity in the curve is called the hemimicelle concentration (HMC) (Figs 2 and 3) which is the point at which hemimicelles just begin to form. They can be thought of as two dimensional aggregates of surfactant molecules on the surface. Hemimicelle formation has been demonstrated from adsorption isotherms under various conditions [12]. Adsorption increases by binding of a second layer of surfactant via hydrophobic interactions, leading to saturation of the surface.

However, according to Koopal *et al.* [13], the strong interactions at low surface coverage which characterizes the HMC cannot be explained by lateral interactions as in micelles. These authors suggest that there are some hydrophobic regions (of the order of a few per cent of the total surface area) on the mainly hydrophilic surface. This has been shown to be the case for silica and quartz. At low levels of surface coverage, adsorption takes place by horizontal binding to hydrophobic regions. Perpendicular adsorption only takes place at higher coverages (around 10%) as a result of inter-chain interactions. For these authors, the breaking point of slope, attributed by Fuerstenau to HMC, occurs before the transition from horizontal to perpendicular binding.

On heterogeneous surfaces, according to Schechter [11], there are sites more favourable to adsorption than others. When a surfactant having a charge opposite to that of the surface adsorbs, only bi-layered aggregates are formed. These bi-layered structures are called admicelles, and are found on a given patch of a heterogeneous surface at a critical solution concentration CAC (critical admicelle concentration) which is specific to that patch. This hypothesis implies that if the surface is homogeneous, the adsorption isotherm consists of a low concentration region in which adsorption increases slowly with concentration, followed by a vertical step to complete bi-layer coverage at the CAC. Adsorption will then remain constant at increasing solution concentrations, since bi-layer coverage represents complete saturation of the surface. Conversely, if the surface is made up of a distribution of patches, with different adsorption energies, the overall isotherm appears as a series of steps in surfactant adsorption.

On the basis of these considerations three points may be made:

(1) horizontal adsorption can occur at low surfactant concentrations;

(2) perpendicular adsorption takes place after the break in slope via the formation of hemi or admicelles;

(3) the plateau in the adsorption isotherm reflects the formation of a bi-layer.

The plateaux in the plots of $(\log I_{corr})^{-1} = f \log (C)$ can thus be attributed to saturation of the surface by the inhibitor, corresponding to zones of CMC (Figs 2 and 3). This is in agreement with the results of Schechter *et al.* [11], and supports the assumption that these curves can be regarded as adsorption isotherms. These S-shaped curves may be accounted for by a process of competitive adsorption [14] via strong interactions of a chemical nature.

The initial protection of cathodic sites observed at low concentrations ($C < 10^{-5}$ M for 2-hexadecyl imidazoline and $< 5 \times 10^{-6}$ M for 2-hexadecyl imidazole) can therefore be attributed to the adsorption of molecules bound horizontally by their polar regions. The hydrophobic chain may also be arranged horizontally as discussed by Koopal *et al.* [13]. The π electrons of the heterocyclic ring bind to the metal surface. The cathodic sites (negatively charged) preferentially bind positively charged inhibitors. The higher efficiency of imidazole, due probably to enhanced adsorption, is a result of the presence of six electrons delocalized over the heterocyclic ring, whereas imidazoline only has four electrons which are restricted to the region between the two N atoms in the ring (Fig. 1).

When the concentrations are higher than those mentioned above, there are mixed anodic and cathodic effects. In this case there is a relative improvement in the protective effect of imidazoline with respect to imidazole. This change occurs in the rising portion of the plots of $(\log I_{corr})^{-1} = f \log (C)$. This can be attributed to a change in the orientation of molecules adsorbed at the interface resulting from hydrophobic interactions between chains. In this situation it is likely that the surfactant molecules bind perpendicularly to the surface. Adsorption via the N atom electron pair takes places at cathodic sites. It can also occur to some extent on anodic sites, especially in the case of imidazoline, where the sp^3 character of the electron pair is strong than for imidazole as the electrons are less delocalized (Fig. 1). The separation between this electron pair and the positively charged ion enables the electron pair to interact with anodic sites (positive).

At increasing concentrations of inhibitor, the carbon chains of the molecules already in place, parallel to the metal surface, change their orientation via hydrophobic effects. This corresponds to the rising section of the $(\log I_{corr})^{-1} = f \log (C)$ plots and the concomitant formation of micelles in the solution. The adsorption plateau is then reached as a bi-layer is formed, the two layers being held together by hydrophobic interactions. The film formed corresponds to saturation of the surface which explains the powerful inhibitory effects observed.

Electrochemical impedance measurements carried out at the corrosion potential and in the anodic and cathodic ranges can provide valuable information about the inhibition mechanism which cannot be obtained from steady-state polarization curves alone:

(i) For concentrations greater than the CMC (5×10^{-5} M) 2-hexadecyl imidazoline and 2-hexadecyl imidazole, as a consequence of their hydrophobic character, mainly form an adherent but thick micellar film. The behaviour differences observed in the cathodic range could be due to a different binding mode of the inhibitor to the metal. Thus in the case of imidazole a flat fixation of the polar head is more likely in view of the π electron delocalization within the cycle. The hypothesis is borne out by the fact that cathodic polarization results in a lowering of interfacial capacity; this reduction is revealed by reinforcement of the inhibiting effect.

(ii) The film acts as a diffusion barrier: this is corroborated by the fact that the current densities near the corrosion potential are greatly reduced, in agreement with a mixed inhibitive action of the compounds. They slow down the rate of transfer of the cations H^+ (or H_2S molecules) toward the metal surface (cathodic behaviour) and change the dissolution rate of the metal (anodic behaviour).

(iii) Over a wide range of potentials around E_{corr} the film seems to have constant properties, as indicated by the stable values of double-layer capacitance.

These three points corroborate a chemical adsorption mechanism of the molecules. Bonding between the molecule investigated and the metal surface is suggested as involving N atoms from the heterocyclic group.

References

[1] P. Dupin, A. de Savignac, A. Lattes, B. Sutter and Ph. Haicour, 5th European Symposium on Corrosion Inhibitors *Ann. Univ. Ferrara* **7** (1980) 301.

[2] P. Dupin, A. de Savignac and A. Lattes, *Materials Chemistry* **6** (1981) 443 and **7** (1982) 549.

[3] S. Cosnier, P. Dupin, A. de Savignac, M. Comtat and A. Lattes, *Electrochim. Acta* **9** (1986) 1213.

[4] A. W. Adamson, 'Physical Chemistry of Surfaces', 4th edn., Wiley, N.Y. (1982) p. 92.

[5] A. de Savignac, T. Kabbage, P. Dupin and M. Calmon, J. *Heterocyclic Chem.* **15** (1978) 897.

[6] C. Gabrielli and M. Keddam, *Electrochim. Acta* **19** (1974) 355.

[7] W. Warburg, *Ann. Physik* (1901) 125.

[8] M. Duprat, A. Srhiri, Y. Derbali and N. Pebere, Proceedings International Symposium "Electrochemical Methods in Corrosion Research", Toulouse (1985) edited by M. Duprat, *Materials Science Forum* **8** (1986) 267.

[9] M. V. Pospelov, A. V. Ignatov, V. V. Yaminskiy and A. V. Fokin, 6th European Symposium on Corrosion Inhibitors, *Ann. Univ. Ferrara* N.S. Seg. V, **8** (1985) 455.

[10] D. W. Fuerstenau and T. Wakamatsu, *Faraday Discuss. Chem. Soc.* **59** (1975) 157.

[11] J. H. Harwell, J. C. Hoskins, R. S. Schechter and W. H. Wade, *Langmuir* **1** (1985) 251.

[12] A. de Savignac, P. Dupin, H. Matondo, S. Bories and A. Lattes, *J. Chem. Techn. Biotechnol.* **30** (1980) 117.

[13] L. K. Koopal and J. J. Ralston, *Colloïd Interface Sci.* **2** (1986) 362.

[14] C. H. Giles, A. P. D'Silva and I. A. Easton, *J. Colloïd Interface Sci.* **3** (1974) 766.

[15] M. Stern and A. L. Geary, *J. Electrochem. Soc.* **104** (1957) 56.